



Concentration of stigmasterol, β -sitosterol and squalene from passion fruit (*Passiflora edulis* Sims.) by-products by supercritical CO₂ adsorption in zeolite 13-X

Luana C. dos Santos^{a,b,*}, Renata G. Broco e Silva^b, Eupidio Scopel^c, Tahmasb Hatami^d, Camila A. Rezende^c, Julian Martínez^b

^a Foodomics Laboratory, Instituto de Investigación en Ciencias de la Alimentación (CIAL, CSIC-UAM), Campus de Cantoblanco, Nicolás Cabrera 9, Madrid 28049, Spain

^b Departamento de Engenharia e Tecnologia de Alimentos, Faculdade de Engenharia de Alimentos, Universidade Estadual de Campinas (UNICAMP), Monteiro Lobato, 80, Campinas, SP 13083-862, Brasil

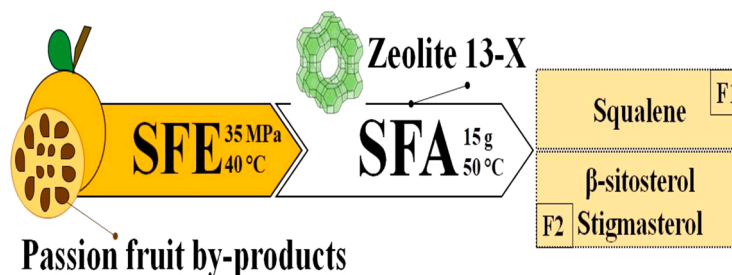
^c Instituto de Química, Universidade Estadual de Campinas (UNICAMP), Josue de Castro s/n, Campinas, SP 13083-970, Brasil

^d Departamento de Engenharia de Materiais e Bioprocessos, Faculdade de Engenharia Química, Universidade Estadual de Campinas (UNICAMP), Av. Albert Einstein 500, Campinas, SP 13083-852, Brasil

HIGHLIGHTS

- Supercritical fractionation of passion fruit by-products extracts using zeolites.
- Different adsorption temperature and zeolite masses were applied.
- Squalene and phytosterols concentration doubled after fractionation (50 °C, 15 g).
- Supercritical fractionation is a clean process to concentrate bioactive compounds.

GRAPHICAL ABSTRACT



ARTICLE INFO

Keywords:

P. edulis by-products
Supercritical fractionation
Zeolite
Phytosterols

ABSTRACT

Phytosterols and squalene, widely applied in pharmaceutical and food industries, were extracted and concentrated from passion fruit by-products (PFBP). A supercritical extraction using CO₂ (SFE) was performed for PFBP, and the obtained extract underwent supercritical fractionation (SFA) (inlet at 35 MPa, 50–70 °C) in a column packed with zeolite 13-X (5–15 g). The extraction and fractionation yields were measured, whereas the composition of the PFBP extract and their fractions was assessed by gas chromatography-mass spectrometry (GC-MS). Fractionated extract recovered presented different trends depending on temperature and zeolite mass combinations, and the highest recovery (approximately 95%) was achieved at 50 °C with 15 g of adsorbent. At the same SFA conditions, the concentration of squalene, β -sitosterol and stigmasterol was twice that obtained in PFBP extract. Finally, SFA proved to be a clean and effective technique to concentrate squalene and phytosterols from PFBP, which should be extended to other food residues.

* Corresponding author at: Foodomics Laboratory, Instituto de Investigación en Ciencias de la Alimentación (CIAL, CSIC-UAM), Campus de Cantoblanco, Nicolás Cabrera 9, Madrid 28049, Spain.

E-mail address: luana.dsantos@csic.es (L.C. dos Santos).

<https://doi.org/10.1016/j.supflu.2024.106250>

Received 26 January 2024; Received in revised form 17 March 2024; Accepted 18 March 2024

Available online 21 March 2024

0896-8446/© 2024 Elsevier B.V. All rights reserved.

1. Introduction

Phytosterols and squalene are bioactive compounds found in plants that have garnered considerable attention from pharmaceutical and food industries. Phytosterols present various beneficial properties, including analgesic, immune-regulating, anti-inflammatory, antioxidant, anticancer, and anti-aging effects, as well as the ability to prevent cardiovascular diseases [1]. Squalene, on the other hand, acts as an antioxidant, promotes skin hydration, serves as an emollient in vaccine adjuvants, exhibits anticancer properties, tumor- and cardio-protective effects, and has the potential to lower serum cholesterol levels [2,3]. Squalene was first isolated from shark liver and could be concentrated up to 95 wt%. However, hunting sharks for squalene extraction has a negative impact on the marine environment and more sustainable sources are currently under investigation. Some plant seeds are considered a rich source of this terpene (e.g., amaranth, accounting for almost 10% of squalene in their seed oil [4]).

Passion fruit by-products (PFBP) are particularly advantageous as phytosterols and squalene sources in Brazil, where the annual production of yellow passion fruit (*Passiflora edulis* Sims.) reaches 700,000 tons and is mainly destined for juice production, resulting in a significant amount of PFBP [5] including the rinds, and a blend of pulp residues and seeds. Squalene and phytosterols can be extracted from the seeds using either organic solvents or supercritical CO₂. Supercritical fluid extraction (SFE), employing environmentally friendly solvents such as CO₂, offers notable benefits including the use of green solvents, mild operating temperatures, high extraction efficiency, excellent selectivity, and easy separation of the extract from the solvent [6].

SFE from PFBP has been previously studied in the literature. Barrales et al. [7] performed SFE from passion fruit seeds and investigated the influence of pressure (16–29 MPa), temperature (38–53 °C), and ultrasonic power (0–800 W) on the extract yield and composition, showing that the application of ultrasonic waves could enhance the SFE global yield by up to 29%. Oliveira et al. [8] compared three different extraction methods, namely SFE, low-pressure extractions (LPE) using cold maceration (MAC), and ultrasound-assisted extraction (UAE) in the recovery of phytosterols and squalene from two types of PFBP, passion fruit seeds and passion fruit seed cake. The results demonstrated that SFE at 25 MPa and 40 °C, as well as MAC with an ethanol-water mixture (1:1, v/v), yielded the highest extraction yields for passion fruit seeds (27%) and passion fruit seed cake (6%), respectively. Delvar et al. [9] tested different extraction methodologies to obtain passion fruit seed oil and reported carotenoid content of 3.2 mg β-carotene equivalent/kg oil in SFE-CO₂ extracts at 20 MPa and 60 °C. Therefore, the pressure increase in this work considerably enhanced the extraction of these compounds by raising solvent density and thus favoring the extraction of molecules with higher hydrophobic chains.

Although SFE itself is a promising technology for PFBP extraction, it can be combined with a suitable fractionation procedure to concentrate or isolate target components. In related work, Viganó et al. [10] suggested that the sequential SFE process of PFBP (composed of pulp residues and seeds) can result in three extract fractions rich in tocopherols, fatty acids, and carotenoids, respectively. To obtain these fractions, temperature and pressure in the first, second, and third steps were 60 °C and 17 MPa, 50 °C and 17 MPa, and 60 °C and 26 MPa, respectively. In another work that used the same raw material, Dos Santos et al. [5] applied a sequential SFE and fractionation with pressure reduction with supercritical CO₂ using two separators in series to obtain fractionated extracts concentrated in δ-tocotrienol, β/γ-tocotrienol, squalene, and carotenoids. For their studies, SFE was fixed at 35 MPa and 40 °C and the pressure and temperature of the separators ranged 17–25 MPa and 50–80 °C, respectively. The authors concentrated squalene about 5.2 times after depressurization of the second separator, but this fraction presented a very low yield (less than 2%). Given this limitation, further exploration of alternative fractionation techniques is warranted.

In addition to combining SFE with fractionation through pressure

reduction, SFE can also be coupled with the adsorption process (SFA) using zeolite, leveraging the advantages of the separation process based on solute solubility, molecular structure, polarity, and size to enhance concentration.

Zeolite are inorganic microporous materials, mainly composed of aluminum, silica, and oxygen, organized by tetrahedrons linked by oxygen atoms in a well-organized molecular structure, forming multidimensional channels. These channels work as a sieve, so that zeolites act as potential adsorbents in concentration or purification processes due to their remarkably high inner surface [11]. The molecular structure plays a crucial role in fractionation. For example, squalene, a triterpene, features a polyunsaturated open-chain molecule structure, while carotenoids have rings at their extremities. This observation suggests that fractionation using zeolite as an adsorbent may be more successful when both compounds are present in the sample compared to processes that solely rely on phase equilibrium as the separation principle.

In a recent study on the combination of SFE and SFA, Hatami et al. [12] explored the sequential integration of SFE with supercritical adsorption (SFA) to obtain a fractionated extract enriched in tocopherols. In the adsorption column, zeolite 13-X, a well-known type of natural zeolite, was chosen due to its high adsorption capacity, commercial availability and relatively low production cost [13,14]. SFE was conducted at 40 °C and 25–35 MPa, while the SFA column, packed with 8 g of zeolite, operated between 40 and 60 °C, yielding a maximum of 55 mg tocopherols/kg of PFBP.

Due to the biomedical advantages of stigmasterol, β-sitosterol, and squalene, the current work aims to advance upon our previous research by investigating the feasibility of concentrating these compounds from PFBP using supercritical CO₂ adsorption on zeolite 13-X. While drawing from the methodology employed by Hatami et al. [12] to concentrate tocopherols, the present work introduces a distinct objective: concentrate phytosterols (stigmasterol and β-sitosterol), and squalene. In order to achieve this goal, the present approach is tackling two technical challenges encountered in previous research: 1) the limited extract quantity obtained in each run due to capacity constraints and low yield from PFBP, hindering accurate composition analysis, and 2) the fractionation dynamics. While overcoming such limitation from an industrial perspective may comprise using two interchangeable extractors [15], which could be economically feasible [16], we propose a modified approach applicable for lab-scale experimentation: initially, we aim to obtain a higher quantity of PFBP extract from SFE. By doing this, it is also possible to ensure a homogenous composition of the extract prior to adsorption fractionation once each compound exhibits its own mass transfer kinetics [10], thus disturbing the fractionation dynamic. Subsequently, we implemented a two-step process involving the solubilization of PFBP extract with supercritical CO₂, followed by selective adsorption on zeolite. The modified method improves upon Hatami et al.'s [12] approach by starting with a higher quantity of PFBP extract for accurate analysis of extract composition, and by using a solubilization column to maintain consistent CO₂ saturation levels once the solid matrix is removed from the system.

2. Materials and methods

2.1. Pre-treatment and characterization of PFBP

The PFBP used in this work were composed of pulp residues and seeds and were kindly donated by the company Sítio do Belo, located in Paraíba, São Paulo, Brazil. The fresh PFBP were dried in an air oven (Marconi MA/035, Piracicaba, SP, Brazil) at 45 ± 5 °C for nearly 36 hours and then ground in a domestic blender to increase the surface area for solvent contact in SFE. The dried and ground PFBP were stored at –18 °C until SFE of the lipid content or physicochemical characterization, which included: i) moisture content (method 931.04, AOAC, 1997), ii) total lipid content using intermittent reflux (Soxhlet) apparatus (method 963.15, AOAC, 1997), iii) protein content using Kjeldahl

method (method 970.22, AOAC, 1997), and iv) total dried ashes (method 972.15, AOAC, 1997). Carbohydrates and fibers were calculated as the corresponding residual amount of material after subtracting moisture, lipid, protein and ashes. In addition, water activity (a_w) was measured in Aqualab (Decagon Devices, Pullman, WA, USA) at 24.7 ± 0.3 °C. Water activity (a_w) measures the available water in PFBP, ranging from 0 to 1, where 1 represents pure water, and it's crucial in food science and microbiology for its impact on food stability, shelf life, and safety.

2.2. Mean particle diameter (D_s), apparent density (ρ_b), real density (ρ_r), bed porosity (ϵ) and adsorbent specific surface area (S_{BET})

Dried and ground PFBP and zeolite 13-X were physically characterized to understand better mass transfer mechanisms in both SFE and SFA processes. The mean particle diameter was determined for PFBP using a set of small sieves from the Tyler series BRINOX (Caxias do Sul, RS, Brazil). The Sauter diameter (D_s) was chosen as the mean representative particle diameter since it is the most recommended in processes where the surface area is relevant, which is the case of SFE. D_s was calculated using Eq. 1.

$$D_s = \frac{1}{\sum_{i=1}^n \frac{x_i}{D_i}} \quad (1)$$

where,

x_i is the mass fraction retained in sieve i , and

D_i is the mean diameter of the particles retained in sieve i .

For the zeolite bed characterization, a more extended characterization was performed. Firstly, the apparent density (ρ_b), which is the ratio between the particulate material mass and its volume, including the void, was measured using the sufficient mass of zeolite (manually compacted) to fill a 10 mL graduated cylinder. The mass was weighted and ρ_b was calculated as the ratio between mass and volume. The real density (ρ_r) was calculated using a gas pycnometer Multivolume Pycnometer 1305 (Micromeritics, Norcross, GA, USA). Therefore, the bed porosity (ϵ) was calculated with Eq. 2.

$$\epsilon = 1 - \left(\frac{\rho_b}{\rho_r} \right) \quad (2)$$

The surface area is an essential parameter in adsorption processes, especially those using porous adsorbents such as zeolite 13-X. The B.E.T. model, developed by Brunauer, Emmet, and Teller [17], was applied for the adsorbent used in this work. Briefly, around 1 g of zeolite 13-X was submitted to heat treatment at 200 °C for two hours and sequentially cooled down at -196 °C under a constant flow of nitrogen in the surface area and porosity analyzer Micromeritics ASAP 2020 (Norcross, GA, USA). The theory of sorption isotherms is used to calculate the adsorbed nitrogen volume in the surface monolayer in a range of relative pressures (P/P_0) lower than 0.03 MPa. Then, the specific surface area is calculated using Eq. 3. In addition, the same analysis allowed the calculation of zeolite 13-X pore diameter and specific pore volume (pore diameter < 1785.5 Å). All the adsorbent characterization assays described in this topic were performed in triplicate.

$$S_{BET} (m^2/g) = \frac{v_m N_s}{V a} \quad (3)$$

where:

S_{BET} is the specific surface area;

v_m is the volume of a monolayer of adsorbed nitrogen

N is the Avogadro's number (6.02×10^{23} molecules/mol);

s is the cross-section of the nitrogen molecule;

V is the molar volume of nitrogen, and

A is the mass of sample.

2.3. Supercritical CO_2 extraction (SFE) of PFBP

The PFBP extract (to be further subjected to SFA) was obtained by SFE with CO_2 as solvent. An optimized SFE condition (35 MPa and 40 °C) was used, with the pressure and temperature applied to obtain the maximum global yield [10]. The solvent-to-feed ratio (S/F) was fixed at 46 kg CO_2 /kg dry PFBP, according to a previous SFE kinetics using the same material [5]. The SFE global yield (x_0) was calculated as the mass ratio between extract (E) and feed (F), according to Eq. 4. This step was crucial to obtain a PFBP extract rich in lipid-soluble compounds. For comparison, a commercial oil (COM) obtained by cold pressing from Campestre Óleos Vegetais (São Bernardo do Campo, SP, Brazil) was also characterized (Section 3.1).

$$x_0 (\%, g/g) = \frac{E}{F} \times 100 \quad (4)$$

2.4. Supercritical CO_2 adsorption (SFA)

SFA of the PFBP extracts was performed in a homemade unit, shown in Fig. 1, which comprises a stainless steel solubilization vessel (200 mL), an air-driven CO_2 pump, one cooling bath, two heating baths and a fractionation column ($L = 65$ cm, i.d. = 8.7 mm) filled with zeolite 13-X. Approximately 3 g of PFBP extract were distributed along 20 sheets of paper towel and inserted in the stainless steel solubilization vessel. This method, which was previously described in the literature [18,19], used the paper towel's capacity of soaking to facilitate efficient and controlled measurement of oil solubility in CO_2 through its ample surface area and uniform distribution. Solubilization was fixed at a CO_2 flow rate of 1.06×10^{-4} kg/s, pressure of 35 ± 2 MPa, temperature of 40 ± 2 °C and static time of 45 minutes once a previous solubility test of the same extract found the best solubility at high CO_2 densities and the established conditions are in the limit of the equipment. After solubilization, the PFBP extract was transferred to the adsorption column filled with 5, 10, or 15 g of compacted zeolite 13-X. The SFA column was immersed in a water bath at 50, 60, or 70 ± 2 °C. Each SFA condition was performed in duplicate. An SFA kinetic run of 300 min at 50 °C using 10 g of zeolite 13-X was previously performed to find the exact time the accumulated mass of the collected fractions remained constant. These fractions were collected at the SFA column outlet in glass flasks after 5, 20, 60, 120, 180, 240, and 300 min. After establishing that 180 min was sufficient to achieve stability, the fractions in the subsequent kinetics were collected at 10, 25, 40, 50, 65, 85, 95, 135, 155, and 180 min. In addition, to verify extract composition effects in SFA, a comparative fractionation kinetics using 10 g of zeolite 13-X and 40 °C was performed for two different extracts: COM and PFBP extract (obtained according to the method described in Section 2.3). The SFA global yield achieved along fractionation kinetics was also calculated using Eq. 4, where feed (F) was the amount of extract subjected to solubilization and E was the amount of fractionated extract collected from the adsorption column outlet.

To enable their characterization (Section 2.5), the collected fractions were separated in F1, which consists of the combined fractions collected during the initial 40-minute period, or F2, comprising the combined fractions collected from 40 to 180 minutes. The pressure drop at the end of the fractionation column was measured in all experiments. The fractions were collected in glass flasks wrapped with aluminum foil to prevent light oxidation and stored under -18 °C until further analysis.

While no attempt was made in this study to regenerate zeolite, it's important to note that for industrial applications, zeolite regeneration is necessary. Methods typically include thermal treatment at high temperatures to decompose adsorbed molecules from the pores, or solvent washing using chemicals like ethanol to dissolve contaminants from the zeolite structure [20,21].

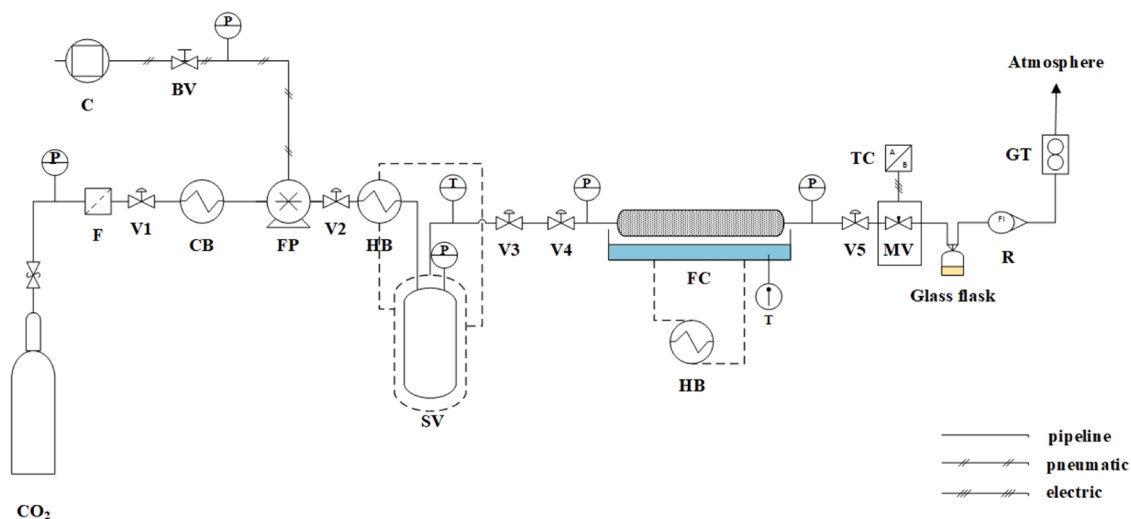


Fig. 1. Flow diagram of SFA of PFBP extract using zeolite 13-X as adsorbent material. Legend: C: air compressor; F: pipeline filter; BV: bypass valve; CB: cooling bath; V1-V5: blocking valves; P: pressure indicators; T: temperature indicators; FP: air-driven CO₂ pump; HB: heating baths; SV: solubilization vessel; FC: adsorption column; MV: micrometer valve; TC: temperature controller; R: rotameter, and GT: gas totalizer.

2.5. Characterization of PFBP extract and their fractions

2.5.1. Total carotenoids

The quantification of carotenoids in the PFBP extract and their fractions obtained by SFA was performed using the method described in Sogi et al. [22] with some modifications. The samples were diluted in hexane at approximately 50 mg/mL. The calibration curve was built in a range of 0.5–5 µg β-carotene/mL. The samples were added into a 96-well microplate and the absorbance was read at $\lambda = 450$ nm in a microplate reader FLUOstar Omega (Bmg Labtech, Ortenberg, Germany). The total carotenoid analyses were performed in triplicate for each sample, and the results are representative of the mean of a process duplicate.

2.5.2. Quantification of squalene, β-Sitosterol and stigmastrol

The quantification of squalene, β-sitosterol, and stigmastrol was performed by gas chromatography coupled to mass spectrometry (GC-MS) according to the methodology of Pokkanta et al. [23], with adaptations. Standard calibration curves of the mentioned compounds were built diluting the standard in dichloromethane from 0.02 to 0.3 mg/mL. Approximately 0.03 g of the extract was diluted in 200 µL of dichloromethane and 1 µL at a split ratio 50:1 was injected in a gas chromatograph Agilent 7890 A (Agilent Technologies, Palo Alto, CA, USA) coupled with a monoquadrupole mass spectrum detector Agilent 5975 C (Agilent Technologies, Palo Alto, CA, USA). The separation column used in the GC-MS was an HP-5MS (30 m × 250 µm × 0.25 µm) from the same manufacturer, and the carrier gas was helium. The flow rate was fixed at 1 mL/min, and the temperature in the injection was 300 °C. After, the temperature was ramped until 200 °C at a constant rate of 15 °C/min and went back to 300 °C slowly, at a rate of 3 °C/min. At the end of the separation, compounds were ionized using an electron ionization source (EI) at 300 °C, in a scan range of 30–550 u. The results were expressed as the mean values ± standard deviation from process duplicates (except for commercial oil that represents mean values from an analysis duplicate) in mg of the compound/kg extract.

2.6. Statistical analysis

The analysis of variance (ANOVA) and Tukey's test at a 95% statistical significance was performed using Statistica 10 (StatSoft, Tulsa, OK, USA) to evaluate the differences in composition of the extract and the SFA fractions.

3. Results and discussion

3.1. Characterization and extraction of PFBP

CO₂ is the most applied solvent in SFE from PFBP, as already reported in the literature [5,7,8,24], since it enables the recovery of a wide range of compounds such as mono- and polyunsaturated fatty acids, carotenoids, tocopherols, etc. Therefore, SFE with CO₂ was selected to obtain an extract rich in lipid-soluble compounds, which was the first step of this work. The SFE global yield and the composition of the PFBP are presented in Table 1.

The physicochemical characterization provides important information (e.g. % of moisture and lipids) when aiming to submit the material to SFE that intends to recover as much quantity of lipid-soluble compounds as possible. For instance, Ningrum et al. [25] performed a detailed characterization of tropical fruits pomace and found for yellow passion fruit residues (seeds and peel), containing 10.79% of moisture, 18.37% of protein, 2.78% of ashes, 48.36% of carbohydrates, and 19.02% of lipids. Barrales et al. [7] also characterized PFBP (seeds and pulp residues), finding for moisture, proteins, lipids, ashes, and carbohydrates, 3.5, 17.7, 24.2, 6.6 and 51.5%, respectively, which are similar to the values found in this work. However, a noticeable difference can be seen in protein content, which could be mainly attributed to changes in fruit and vegetable crops mainly affected by climate factors. Nonetheless, the most important information to be considered in this work are the lipid fraction and moisture content, which could negatively influence the mass transfer process in SFE. Belwal et al. [26] highlighted

Table 1
Physicochemical characterization of passion fruit by-products (PFBP).

	Dried and milled PFBP
(%, g/g w.b.)	
a_w	0.44 ± 0.02
Moisture	7.3 ± 0.3*
Protein	14.2 ± 0.4
Lipids (Soxhlet)	19.7 ± 0.4
Ashes	2.1 ± 0.1
Carbohydrates and fibers	56.7 ± 0.5
SFE global yield	18.5 ± 0.5
D _s (mm)	1.7 ± 0.1
ϵ	0.40 ± 0.04

a_w : the water activity. D_s: Mean particle diameter. *the moisture of the fresh sample was 55.1 ± 2.4% (w.b., g/g).

moisture as one of the primary data observed in vegetable matrices prior to SFE. In addition, these authors stated that a low a_w can considerably enlarge the storage period, mainly due to the reduction of the enzymatic activity, preventing the degradation of bioactive compounds.

In order to enhance mass transfer process, the particle size of PFBP was reduced, and, their mean particle diameter and bed porosity were measured (Table 1). Despite smaller diameters (≈ 0.74 mm) are preferred to enhance mass transfer [7,10], the PFBP in this work could not be more intensely ground since shear forces induced the release of the lipid content from the seeds as a consequence of the heat generated by the friction between particles. With a particle size of 1.7 mm, the highest possible yield is likely achieved because the SFE yield obtained in this work at 40°C and 35 MPa, 18.5, is close to that obtained by Viganó et al. [10] at the same temperature and pressure but with a particle size of 0.74 mm. In general, determining the optimal particle size requires an optimization task because increasing the grinding time of raw materials in the mill has dual effects on the SFE yield: it enhances yield by reducing particle size and increasing mass transfer area, but it also elevates temperature, accelerating the evaporation rate of volatile materials and potentially decreasing yield [27,28].

The lipid-soluble compounds of interest in this work were also quantified in PFBP extract and in COM so that their concentrations before and after fractionation could be compared (Table 2).

The PFBP extract is richer than the commercial passion fruit seed oil in all the analyzed compounds. Regarding carotenoids, Serra et al. (2019) did not find quantifiable carotenoids in samples of passion fruit seed oil obtained by cold pressing. Surlehan et al. [29] used surfactant-assisted extraction of passion fruit seeds, obtaining 646 mg squalene/kg of extract, which is less than the content obtained in this work. In a previous work of this research group, Dos Santos et al. [5] concentrated squalene using supercritical CO₂ through pressure reduction in a process of SFE with fractional separation. However, they concluded that elevated CO₂ densities are not selective for squalene, and other methods should be considered to separate this compound. Finally, regarding phytosterols, stigmasterol and β -sitosterol present very similar molecular structures, which hampers their separation in any scale larger than analytical. Rotta et al. [30] found concentrations of stigmasterol and β -sitosterol around 800 and 1000 mg/kg, respectively, for yellow passion fruit seed oil obtained by ultrasound assisted extraction. In general, the individual quantification of each compound would be very supportive in the following discussion regarding concentration by SFA.

3.2. Adsorbent characterization

The physical characterization of the zeolite 13-X was obtained from bulk density methods and the physisorption of nitrogen assays, as presented in Table 3.

The characteristics of the adsorbent agree with those reported by Pasquel-Reátegui et al. [14], who used the same zeolite to fractionate compounds from copaiba oleoresin with supercritical CO₂. It is worth noting that zeolite have a surface area over 4 times higher than other

Table 2

Concentration of target compounds obtained by SFE from PFBP and in the commercial oil.

Compound	Concentration (mg/kg extract)		Molecular weight (g/mol)
	SFE	COM	
β -Sitosterol	356 \pm 32	n.q.	414.71
Stigmasterol	277 \pm 17	n.q.	412.69
Squalene	806 \pm 110	482.7 \pm 0.4	410.73
Total carotenoids	25.97 \pm 0.65	n.q.	536.87
(β -Carotene equivalent)			

n.q.: not quantifiable.

Table 3

Physical characterization of zeolite 13-X.

	Zeolite 13-X
B.E.T. surface area (m ² /g)	493 \pm 68
Pore diameter (Å)	25.5 \pm 0.9
Specific pore volume (< 1785.5 Å) (cm ³ /g)	0.31 \pm 0.03
ρ_{apparent} (kg/m ³)	0.72 \pm 0.02
ρ_{real} (kg/m ³)	2.04 \pm 0.01
ϵ	0.65 \pm 0.01

adsorbents like alumina [31], which makes them excellent candidates for a more selective separation of target compounds. In addition, the bed porosity of zeolites is smaller than those of other adsorbents such as aluminum and silicon oxides [14]. Such data is relevant, since more compacted beds will offer high resistance to fluid flow, resulting in long adsorption kinetics.

3.3. Supercritical CO₂ adsorption

3.3.1. Preliminary kinetics and global yield

As mentioned in Section 2.4, SFA kinetics of extracts with different compositions (PFBP extract and COM) were performed. Although remarkable differences in their concentrations were observed (Table 2), there were no significant differences in the SFA global yield, which remained at approximately 28% (Figure S1, supplementary material). Hence, SFA kinetics for PFBP extract is more likely affected by the solvent properties than by the molecular concentration or size of their compounds. The focus on the initial 80 minutes in Figure S1 allows for a concise comparison of the early-stage fractionation kinetics, which exhibit more dynamic behavior compared to the later stages.

A preliminary long-time kinetics (300 min) was performed to determine the time needed to achieve the equilibrium global yield of the PFBP fractionated extract collected from the adsorption column outlet. Figure S2 illustrates the SFA kinetics of PFBP extract using 10 g of zeolite 13-X at 50 °C, upholding a solubilization of the PFBP extract at 35 MPa and 40 °C. Based on the information provided by Figure S2, it can be inferred that the SFA process is practically complete after 180 min, and subsequent fractionation from 180 to 300 min does not affect the global yield of the fractions. Also, according to this kinetics, in the first 40 min, the zeolite is apparently not saturated yet (faster kinetics or higher fractionated extract yields), starting to slow down at this point, when heavier molecules should desorb (slower kinetics or smaller fractionated extract yields). Therefore, the further SFA kinetics presented in Section 3.3.2 ended at 180 min.

3.3.2. SFA kinetics: impact of temperature and adsorbent mass

The impact of temperature and mass of adsorbent in SFA was assessed by analyzing the behavior of PFBP extract fractionation kinetics. Determining the influence of these parameters is crucial, as they directly affect the amount of recovered extract, thereby influencing the concentration of the target compounds (phytosterols and squalene) in the fractions. Additionally, the investigation of SFA kinetics aimed to provide insights into the adsorption and desorption behavior of the lipid-soluble molecules present in the PFBP extract on a microporous material, specifically zeolite 13-X. It is worth noting that information on this subject in literature is scarce.

Fig. 2 shows the influence of temperature and adsorbent mass on the SFA process, whereas Table 4 and Fig. 3 present the recovery of the global fractionated extract and its fractions (F1 and F2), respectively. In all the curves plotted in Fig. 2, the accumulated mass of fractionated extract has an initial linear increase during the first 40–50 min, followed by a shallower ascending trend until it reaches a plateau. As observed in Fig. 2, the kinetics present different trends depending on the combination of adsorption temperature and zeolite mass, and the highest global fractionated extract recovery was about 95% (Table 4) of the initial mass

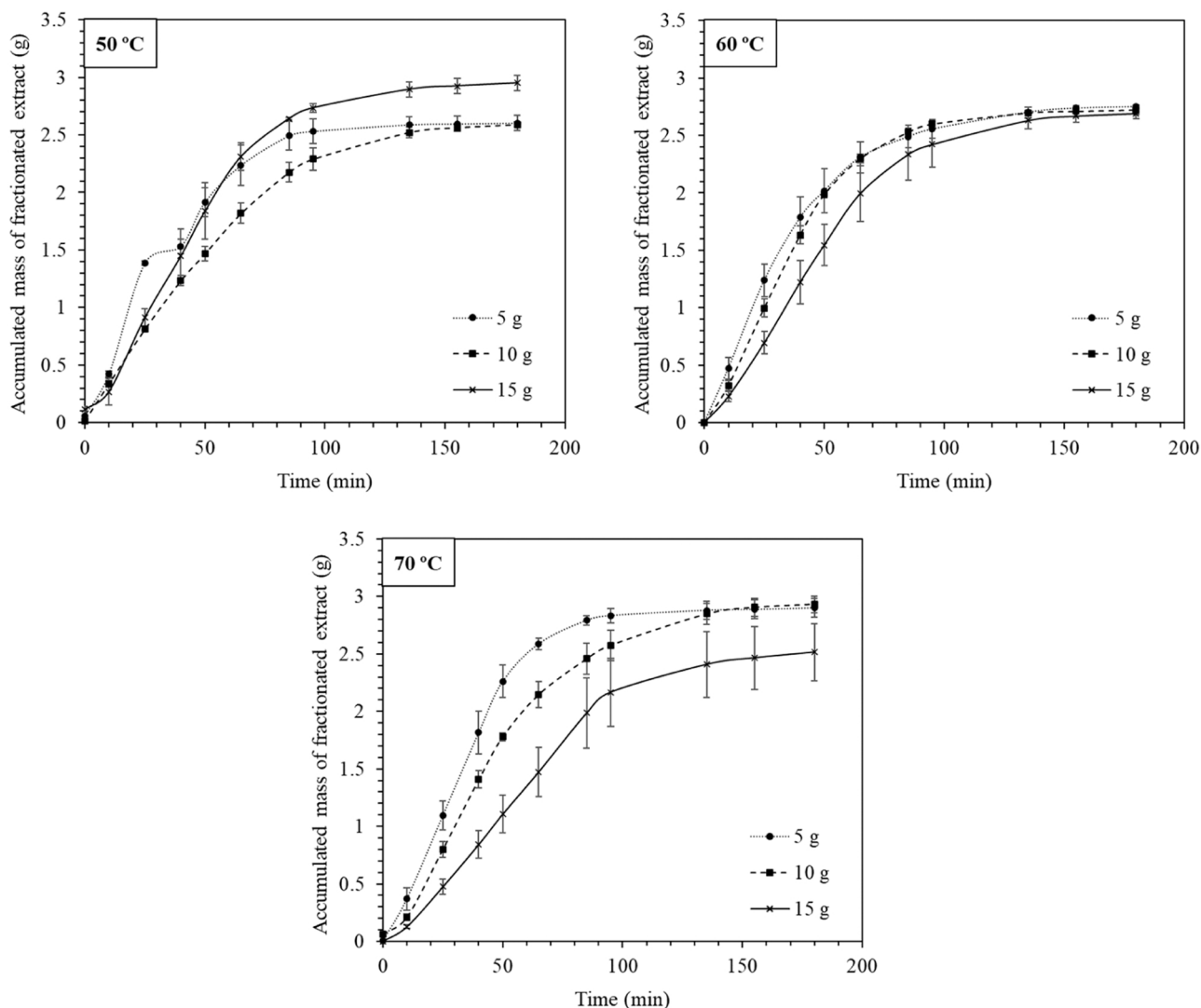


Fig. 2. SFA kinetics of PFBP extract under different temperatures using 5, 10, and 15 g of zeolite 13-X.

Table 4

Supercritical fractionation (SFA) global yield and pressure drop of SFA of PFBP extract with zeolite 13-X.

Mass of zeolite 13-X (g)	Temperature (°C)	SFA global yield (%)	ΔP ($P_1 - P_2$) (MPa)
5 g	50	84 ± 2^a	1.00 ± 0.05
	60	90.1 ± 0.5^a	
	70	93.0 ± 0.8^a	
10 g	50	90.4 ± 0.8^a	2.00 ± 0.05
	60	90 ± 1^a	
	70	92 ± 1^a	
15 g	50	95 ± 2^a	5.00 ± 0.05
	60	90 ± 1^a	
	70	81 ± 7^a	

Equal letters in the same column indicate no significant difference between mean values ($\alpha = 0.05$). ΔP = Pressure drop; P_1 = Solubilization pressure (35 MPa); P_2 = Pressure at the outlet of the SFA column.

of PFBP extract, and it was achieved at 50 °C using 15 g of zeolite 13-X. The observed phenomenon, in which greater adsorption occurs at lower temperatures for smaller amounts of zeolite and at higher temperatures for larger amounts of zeolite, can be attributed to the interplay between adsorption capacity and PFBP extract solubility in supercritical CO₂. Greater amounts of zeolite (15 g) increase the available adsorption sites

on their surface. At higher temperatures, such as 70 °C, the PFBP extract solubility in supercritical CO₂ is reduced [19]. As a result, more adsorption sites can effectively capture and adsorb a higher quantity of molecules. However, when a smaller amount of zeolite (5 g) is used, the available adsorption sites on their surface are limited. At higher temperatures (70 °C), with lower extract solubility in supercritical CO₂, part of the extract cannot be adsorbed on the zeolite surface. This extract will later dissolve back in the supercritical CO₂ that enters the SFA column, reducing the adsorption at higher temperatures. Such results are in accordance with those obtained by Hatami et al. [12], also for PFBP extract. These authors used a similar fractionation system (SFE and SFA processes were performed online) and found lower global fractionated extract masses at higher adsorption temperatures (60 °C), pointing out that decreasing the CO₂ density had a major influence in that case.

Pressure drop was also monitored along SFA, as reported in Table 4. The results indicate that the resistance of the adsorbent increases from 1 MPa when using 5 g of zeolite to 2 MPa when using 10 g of zeolite. However, a significant increase in pressure drop is observed, reaching 5 MPa, as the zeolite mass increases from 10 g to 15 g. These pressure drop findings provide evidence that CO₂ remains in the supercritical state throughout the adsorption column.

Fig. 3 presents the recoveries (in terms of the total PFBP extract used in the solubilization vessel prior to SFA) of fractions F1 and F2 at the evaluated SFA temperatures and masses of zeolite. In Fig. 3(a), F1

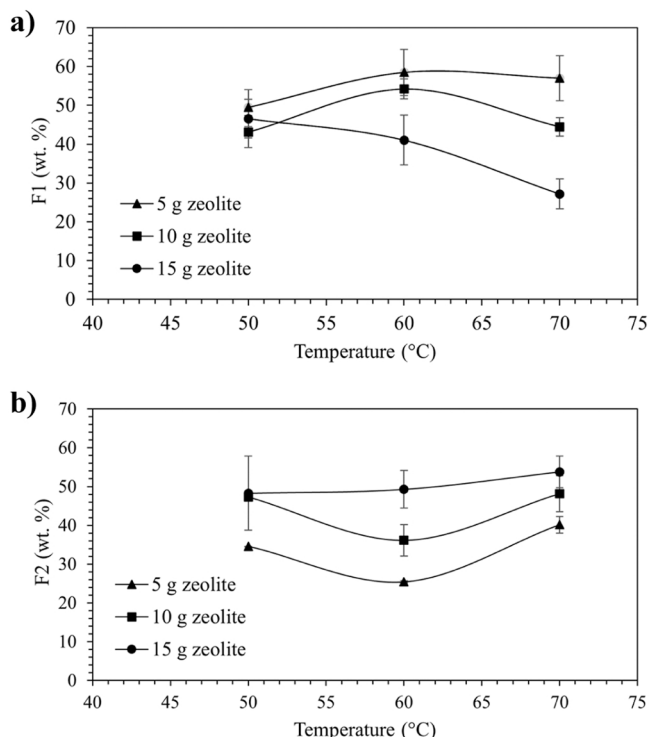


Fig. 3. Recovery of fractions F1 (a) and F2 (b) in terms of the total PFBP extract (≈ 3 g) used in SFA.

recoveries are very similar at 50 °C and decrease with increasing zeolite mass at 60 and 70 °C, which can be explained by the higher surface area of zeolite promoting the adsorption of additional molecules from PFBP extract. On the other hand, Fig. 3(b) shows that F2 recovery increases with zeolite mass for all the applied temperatures, indicating a greater accessibility of the adsorbed solutes into the supercritical CO₂ may occur when the adsorbent is less saturated.

In SFA with 5 and 10 g of zeolite, depicted in Fig. 3(a), the F1 recovery curves exhibit an upward trend as the temperature increases from 50 to 60 °C and decline as the temperature further rises to 70 °C. Conversely, the F1 recovery curve for 15 g of zeolite consistently decreases with increasing temperature. A similar pattern, but with an opposite trend, is observed in Fig. 3(b). With 5 and 10 g of zeolite, the F2 recoveries decline as temperature increases from 50 to 60 °C, reaching a minimum at 60 °C. Conversely, the F2 recovery curve for 10 and 15 g of zeolite slightly increases from 60 to 70 °C, evidencing the effects of CO₂ density, where the lower solubility of the extract and the higher number of available sites were predominant. The sum of F1 and F2 recoveries is equal to the fractionated PFBP extract recovery reported in Table 4.

3.4. Extract characterization

In the present work, we aimed to compare compositions of fractionated extracts obtained under the same temperature (50 °C) and different adsorbent amounts. The selection of such conditions is supported by the findings of Chuang et al. [32], who investigated sterol diffusion mechanisms on zeolite adsorption and reported that temperature had little influence on the selectivity of campesterol, cholesterol and β -sitosterol. Moreover, 50 °C was the lowest temperature applied in our SFA process; thus, less energy is demanded. Finally, isothermal conditions allowed observing the influence of the adsorbent bed to a higher extent.

3.4.1. Total carotenoids

The fractions F1 and F2 were not quantifiable for carotenoids,

explaining why such compounds did not join the same fractionation interest as squalene and phytosterols. The lowest concentration in the calibration curve (Figure S3 in supplementary material) used was 0.5 μ g β -carotene equivalent/mL, and all extracts diluted at 100 mg extract/mL did not reach the respective absorbance. Hence, the SFA of the PFBP had effectively retained the carotenoids in the zeolite. After the first 5 min of SFA kinetics, the extract presented a less intense yellow color than the feed (Figure S4 in supplementary material), showing that the adsorption of such molecules in zeolite 13-X is a rapid process. In contrast, the releasing of these molecules into the supercritical CO₂ is difficult since no dark yellow/orange color was observed in the extracts even after a long time (180 min).

The two main carotenoids found in PFBP extracts obtained by SFE with CO₂ were previously identified as β -carotene and β -cryptoxanthin [10]. The large carbon chain of such molecules (40 carbons) has possibly hampered their passing through the microporous zeolite bed, thus keeping these molecules retained in the adsorption column. Nga et al. [33] investigated the influence of adsorbents composed mainly of silica and alumina iron oxides (clay modified by zero-valent iron) in the removal of β -carotene from palm oil, finding pore diffusion and physisorption as important parameters in carotenoid adsorption in molecular sieves. For the mentioned clay, the authors found an adsorption efficiency of almost 100% of the carotenoid. From the results, zeolites seem to exhibit similar behavior.

3.4.2. Quantification of Squalene, β -sitosterol, and Stigmasterol

GC-MS was performed to quantify squalene and sterols in the fractionated PFBP extract. Fig. 4 presents the composition of the fractions obtained by SFA at 50 °C.

The SFA process with 15 g of zeolite was the best to concentrate all phytosterols and squalene at 50 °C. In comparison to the PFBP extract composition (Table 2), SFA has successfully concentrated squalene, β -sitosterol and stigmasterol in 2.02, 2.03, and 2.25 times, respectively. Overall, the higher the mass of the adsorbent, the higher the mass of the compound to be desorbed and collected at the end of the SFA process. This is confirmed by the highest concentration of sterols recovered in long fractionation times. The concentrations of target compounds achieved with 15 g of zeolite were about two times higher than those obtained using 5 g of zeolite (Fig. 4). The fractionated extracts presented a slight tendency to concentrate phytosterols in F2.

On the contrary, squalene showed rapid fractionation kinetics, being desorbed in the first 40 min of SFA (F1). Since the carbon chains of such molecules (squalene, stigmasterol and β -sitosterol) are very similar, it is probable that differences in their molecular polarities (presence of -OH groups in sterols and absence in squalene) have influenced the pore

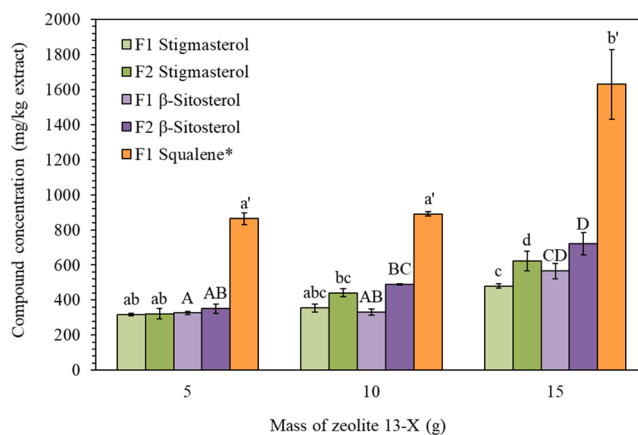


Fig. 4. Concentration of phytosterols and squalene in the PFBP extract fractions after adsorption process at 50 °C and different mass of adsorbent (*F2 Squalene: not quantifiable). Equal formatted letters indicate no significant difference between mean values ($\alpha=0.05$).

diffusion in zeolites and, therefore, resulted in the observed differences in retention along the adsorbent. This result is corroborated by Berezin et al. [34], who states that the adsorption of sterols in zeolite is more likely related to size selectivity. From this point of view, stigmaterol and β -sitosterol are very alike, so similar separation kinetics would be expected for both in zeolites. Chuang et al. [32] presented a diffusion mechanism of sterols in zeolites. They prepared a blend of sterols in hexane and concluded that adsorption is much better controlled by macropore diffusion than by micropore in an irreversible system, which could help the discussion of our results, even though different carrier solvents were used.

Similarly, resin adsorption kinetics was investigated by Yuangsawad et al. [35] for stigmaterol in *n*-heptane. Their results indicated a better prediction by a pseudo-second-order model, in which parameter estimation should combine adsorption and desorption effects. Nonetheless, the resin used in their work had a specific surface area of $224 \cdot 10^{-6} \text{ m}^2/\text{g}$, whereas the zeolite used in this work presented a higher surface area ($493 \text{ m}^2/\text{g}$) (Table 3), meaning that the stigmaterol diffusion model could assist as an indicative but not as a comparable data, and studies on diffusion of stigmaterol in zeolites are necessary.

Compared with fractionation by pressure reduction, SFA seems more efficient. In previous fractionation work, dos Santos et al. [5] aimed to concentrate squalene from the same PFBP used in this work by pressure reduction with two separators connected in series, also using supercritical CO_2 . The fraction with the highest content of squalene was achieved at the end of the separation, reaching concentrations up to around 4800 mg/kg extract. However, the fraction yield was only 9.71% of the extract, whereas in this work it achieved about 47% (Fig. 3a) in the most concentrated fraction, favoring the reduction of the potential production cost of such fractions.

4. Conclusion

This work is mainly dedicated to fractionation processes (using supercritical CO_2) of PFBP extract to obtain concentrated fractions in stigmaterol, β -sitosterol and squalene. The recovery of the extract fractions was assessed at different SFA temperatures and zeolite 13-X masses. The highest extract recovery (95%) was achieved at an adsorption temperature of 50 °C using 15 g of zeolite. At higher temperatures (60 and 70 °C), increasing zeolite mass leads to a decrease in F1 recovery, attributed to enhanced adsorption due to increased surface area. Conversely, the same adsorption condition results in increased F2 recovery, indicating intensified adsorbed solute releasing due to lower saturation of the adsorbents. Stigmaterol, β -sitosterol and squalene were successfully concentrated in fractions obtained at 50 °C and 15 g of zeolite, where concentrations of these compounds doubled in comparison to the initial PFBP extract, being F1 rich in squalene and F2 in stigmaterol and β -sitosterol. The findings provide valuable insights for optimizing the extraction and fractionation processes of phytosterols and squalene from passion fruit by-products.

CRedit authorship contribution statement

Luana C. dos Santos: Writing – original draft, Supervision, Investigation, Formal analysis, Data curation, Conceptualization. **Renata G. Broco e Silva:** Validation, Methodology, Data curation. **Eupidio Scopel:** Methodology, Data curation. **Tahmasb Hatami:** Writing – review & editing, Methodology, Formal analysis. **Camila A. Rezende:** Writing – review & editing, Methodology. **Julian Martínez:** Writing – review & editing, Supervision, Project administration, Funding acquisition, Conceptualization.

Declaration of Competing Interest

The authors declare that they have no known competing financial interests or personal relationships that could have appeared to influence

the work reported in this paper.

Data Availability

Data will be made available on request.

Acknowledgements

The authors thank the São Paulo Research Foundation (FAPESP), Brazil (Process numbers 2018/20700–0, 2019/19360–3, 2021/01008–1 and 2021/12071–6), the National Council for Scientific and Technological Development (CNPq), Brazil (Grant 302968/20229), and the Coordination of Superior Level Staff Improvement – Brazil (CAPES) –Finance Code 001.

Appendix A. Supporting information

Supplementary data associated with this article can be found in the online version at [doi:10.1016/j.supflu.2024.106250](https://doi.org/10.1016/j.supflu.2024.106250).

References

- [1] R. Zhang, Y. Han, D.J. McClements, D. Xu, S. Chen, Production, characterization, delivery, and cholesterol-lowering mechanism of phytosterols: a review, *J. Agric. Food Chem.* 70 (2022) 2483–2494, <https://doi.org/10.1021/acs.jafc.1c07390>.
- [2] M. Spanova, G. Daum, Squalene - biochemistry, molecular biology, process biotechnology, and applications, *Eur. J. Lipid Sci. Technol.* 113 (2011) 1299–1320, <https://doi.org/10.1002/ejlt.201100203>.
- [3] A. Mendes, J. Azevedo-Silva, J.C. Fernandes, From sharks to yeasts: squalene in the development of vaccine adjuvants, *Pharmaceuticals* 15 (2022), <https://doi.org/10.3390/ph15030265>.
- [4] S. Srivastava, Y.N. Sreerama, U. Dharmaraj, Effect of processing on squalene content of grain amaranth fractions, *J. Cereal Sci.* 100 (2021) 103218, <https://doi.org/10.1016/j.jcs.2021.103218>.
- [5] L.C. dos Santos, J.C.F. Johnner, E. Scopel, P.V.A. Pontes, A.P.B. Ribeiro, G.L. Zabot, E.A.C. Batista, M.A.A. Meireles, J. Martínez, Integrated supercritical CO_2 extraction and fractionation of passion fruit (*Passiflora edulis* Sims) by-products, *J. Supercrit. Fluids* 168 (2021), <https://doi.org/10.1016/j.supflu.2020.105093>.
- [6] E. Reverchon, I. De Marco, Supercritical fluid extraction and fractionation of natural matter, *J. Supercrit. Fluids* 38 (2006) 146–166, <https://doi.org/10.1016/j.supflu.2006.03.020>.
- [7] F.M. Barrales, C.A. Rezende, J. Martínez, Supercritical CO_2 extraction of passion fruit (*Passiflora edulis* sp.) seed oil assisted by ultrasound, *J. Supercrit. Fluids* 104 (2015) 183–192, <https://doi.org/10.1016/j.supflu.2015.06.006>.
- [8] D.A. Oliveira, M. Angonese, C. Gomes, S.R.S. Ferreira, Valorization of passion fruit (*Passiflora edulis* sp.) by-products: Sustainable recovery and biological activities, *J. Supercrit. Fluids* 111 (2016) 55–62, <https://doi.org/10.1016/j.supflu.2016.01.010>.
- [9] A. Delvar, P. de Caro, Y. Caro, A. Shum Cheong Sing, R. Thomas, C. Raynaud, Semi-siccative oils and bioactive fractions isolated from reunion island fruit co-product: two case studies, *Eur. J. Lipid Sci. Technol.* 121 (2019) 1–9, <https://doi.org/10.1002/ejlt.201800391>.
- [10] J. Viganó, J.P. Coutinho, D.S. Souza, N.A.F. Baroni, H.T. Godoy, J.A. Macedo, J. Martínez, Exploring the selectivity of supercritical CO_2 to obtain nonpolar fractions of passion fruit bagasse extracts, *J. Supercrit. Fluids* 110 (2016) 1–10, <https://doi.org/10.1016/j.supflu.2015.12.001>.
- [11] Y. Kamimura, M. Shimomura, A. Endo, CO_2 adsorption-desorption properties of zeolite beta prepared from OSDA-free synthesis, *Microporous Mesoporous Mater.* 219 (2016) 125–133, <https://doi.org/10.1016/j.micromeso.2015.07.033>.
- [12] T. Hatami, L.C. dos Santos, G.L. Zabot, P.V. de, A. Pontes, E.A.C. Batista, L.H.I. Mei, I. Mei, J. Martínez, Integrated supercritical extraction and supercritical adsorption processes from passion fruit by-product: experimental and economic analyses, *J. Supercrit. Fluids* 162 (2020) 104856, <https://doi.org/10.1016/j.supflu.2020.104856>.
- [13] E. Pérez-Botella, S. Valencia, F. Rey, Zeolites in adsorption processes: state of the art and future prospects, *Chem. Rev.* 122 (2022) 17647–17695, <https://doi.org/10.1021/acs.chemrev.2c00140>.
- [14] J.L. Pasquel-Reategui, L.C. dos Santos, F.M. Barrales, V.L. Grober, M.B. Soares Forte, A. Sartoratto, C.L. Queiroga, J. Martínez, Fractionation of sesquiterpenes and diterpenic acids from copaiba (*Copaifera officinalis*) oleoresin using supercritical adsorption, *J. Supercrit. Fluids* 184 (2022) 0–2, <https://doi.org/10.1016/j.supflu.2022.105565>.
- [15] T. Hatami, O.N. Ciftci, A step-by-step techno-economic analysis of supercritical carbon dioxide extraction of lycopene from tomato processing waste, *J. Food Eng.* 357 (2023) 111639, <https://doi.org/10.1016/j.jfoodeng.2023.111639>.
- [16] T. Hatami, O.N. Ciftci, Techno-economic sensitivity assessment for supercritical CO_2 extraction of lycopene from tomato processing waste, *J. Supercrit. Fluids* 204 (2024) 106109, <https://doi.org/10.1016/j.supflu.2023.106109>.

- [17] S. Brunauer, P.H. Emmett, E. Teller, Adsorption of Gases in Multimolecular Layers, *J. Am. Chem. Soc.* 60 (1938) 309–319.
- [18] R.G. Bitencourt, N.J. Ferreira, A.L. Oliveira, F.A. Cabral, A.J.A. Meirelles, High pressure phase equilibrium of the crude green coffee oil – CO₂ – ethanol system and the oil bioactive compounds, *J. Supercrit. Fluids* 133 (2018) 49–57, <https://doi.org/10.1016/j.supflu.2017.09.017>.
- [19] L.C. dos Santos, R.G. Bitencourt, P. dos Santos, P. de, T. Vieira e Rosa, J. Martínez, Solubility of passion fruit (*Passiflora edulis* Sims) seed oil in supercritical CO₂, *Fluid Phase Equilib.* 493 (2019) 174–180, <https://doi.org/10.1016/j.fluid.2019.04.002>.
- [20] Ç. Sayilgan, M. Mobedi, S. Ülkü, Effect of regeneration temperature on adsorption equilibria and mass diffusivity of zeolite 13x-water pair, *Microporous Mesoporous Mater.* 224 (2016) 9–16, <https://doi.org/10.1016/j.micromeso.2015.10.041>.
- [21] M. Andrunik, M. Skalny, M. Gajewska, M. Marzec, T. Bajda, Comparison of pesticide adsorption efficiencies of zeolites and zeolite-carbon composites and their regeneration possibilities, *Heliyon* 9 (2023) e20572, <https://doi.org/10.1016/j.heliyon.2023.e20572>.
- [22] D.S. Sogi, M. Siddiq, K.D. Dolan, Total phenolics, carotenoids and antioxidant properties of Tommy Atkin mango cubes as affected by drying techniques, *LWT - Food Sci. Technol.* 62 (2015) 564–568, <https://doi.org/10.1016/j.lwt.2014.04.015>.
- [23] P. Pokkanta, P. Sookwong, M. Tanang, S. Setchaiyan, P. Boontakham, S. Mahatheeranont, Simultaneous determination of tocopherols, γ -oryzanol, phytosterols, squalene, cholecalciferol and phyloquinone in rice bran and vegetable oil samples, *Food Chem.* 271 (2019) 630–638, <https://doi.org/10.1016/j.foodchem.2018.07.225>.
- [24] S. Liu, F. Yang, C. Zhang, H. Ji, P. Hong, C. Deng, Optimization of process parameters for supercritical carbon dioxide extraction of *Passiflora* seed oil by response surface methodology, *J. Supercrit. Fluids* 48 (2009) 9–14, <https://doi.org/10.1016/j.supflu.2008.09.013>.
- [25] A. Ningrum, Supriyadi, S. Anggrahini, L.D. Kusumaningrum, M.W. Hapsari, M. Schreiner, Valorization of food by product from selected tropical fruits pomace, *IOP Conf. Ser. Earth Environ. Sci.* 205 (2018), <https://doi.org/10.1088/1755-1315/205/1/012034>.
- [26] T. Belwal, S.M. Ezzat, L. Rastrelli, I.D. Bhatt, M. Daglia, A. Baldi, H.P. Devkota, I. E. Orhan, J.K. Patra, G. Das, C. Anandharamkrishnan, L. Gomez-Gomez, S. F. Nabavi, S.M. Nabavi, A.G. Atanasov, A critical analysis of extraction techniques used for botanicals: Trends, priorities, industrial uses and optimization strategies, *TrAC - Trends Anal. Chem.* 100 (2018) 82–102, <https://doi.org/10.1016/j.trac.2017.12.018>.
- [27] T. Hatami, J.C.F. Johnner, M.A.A. Meireles, Investigating the effects of grinding time and grinding load on content of terpenes in extract from fennel obtained by supercritical fluid extraction, *Ind. Crops Prod.* 109 (2017) 85–91, <https://doi.org/10.1016/j.indcrop.2017.08.010>.
- [28] J.C.F. Johnner, T. Hatami, G.L. Zabet, M.A.A. Meireles, Kinetic behavior and economic evaluation of supercritical fluid extraction of oil from pequi (*Caryocar brasiliense*) for various grinding times and solvent flow rates, *J. Supercrit. Fluids* 140 (2018) 188–195, <https://doi.org/10.1016/j.supflu.2018.06.016>.
- [29] H.F. Surlehan, Noor Azman N.A, R. Zakaria, N.A. Mohd Amin, Extraction of oil from passion fruit seeds using surfactant-assisted aqueous extraction, *Food Res* 3 (2019) 348–356, [https://doi.org/10.26656/fr.2017.3\(4\).146](https://doi.org/10.26656/fr.2017.3(4).146).
- [30] E.M. Rotta, M.C. Da Silva, L. Maldaner, J.V. Visentainer, Ultrasound-assisted saponification coupled with gas chromatography-flame ionization detection for the determination of phytosterols from passion fruit seed oil, *J. Braz. Chem. Soc.* 29 (2018) 579–586, <https://doi.org/10.21577/0103-5053.20170170>.
- [31] A.A. Bankole, V. Poulouse, T. Ramachandran, F. Hamed, T. Thiemann, Comparative study of the selective sorption of organic dyes on inorganic materials—a cost-effective method for waste treatment in educational and small research laboratories, *Separations* 9 (2022), <https://doi.org/10.3390/separations9060144>.
- [32] Y.H. Chuang, Y.H. Ju, A. Widjaja, Kinetic studies of phytosterol adsorption on zeolite, *Sep. Sci. Technol.* 42 (2007) 611–624, <https://doi.org/10.1080/01496390601070182>.
- [33] J. Nga, J. Avom, J. Tonga Limbe, D. Ndinteh, H.L. Assonfack, C.M. Kede, Kinetics and thermodynamics of β -carotene adsorption onto acid-activated clays modified by zero valent iron, *J. Chem.* 2022 (2022) 17–19, <https://doi.org/10.1155/2022/6505556>.
- [34] M.Y. Berezin, J.M. Dzenitis, B.M. Hughes, S.V. Ho, Separation of sterols using zeolites, *Phys. Chem. Chem. Phys.* 3 (2001) 2184–2189, <https://doi.org/10.1039/b100239m>.
- [35] R. Yuangsawad, S. Sinpichai, T. Bhamarasuta, C. Ladadok, S. Panchanon, D. Naranon, Kinetics and Equilibrium Modeling of Sterol Adsorption on Styrene-divinylbenzene Cation-exchange Resins, *Chem. Eng. Technol.* 42 (2019) 940–946, <https://doi.org/10.1002/ceat.201800608>.